A Closer Comparison of Early and Late-Winter Atmospheric Trends in the Northern Hemisphere

YONGYUN HU

NASA Goddard Institute for Space Studies, and Center for Climate Systems Research, Columbia University, New York, New York, and MOE Key Laboratory of Severe Storm and Flood Disasters, Department of Atmospheric Sciences, Peking University, Beijing, China

KA KIT TUNG

Department of Applied Mathematics, University of Washington, Seattle, Washington

JIPING LIU

School of Earth and Atmospheric Sciences, Georgia Institute of Technology, Atlanta, Georgia

(Manuscript received 14 April 2004, in final form 28 July 2004)

ABSTRACT

Decadal trends are compared in various fields between Northern Hemisphere early winter, November–December (ND), and late-winter, February–March (FM), months using reanalysis data. It is found that in the extratropics and polar region the decadal trends display nearly opposite tendencies between ND and FM during the period from 1979 to 2003. Dynamical trends in late winter (FM) reveal that the polar vortex has become stronger and much colder and wave fluxes from the troposphere to the stratosphere are weaker, consistent with the positive trend of the Arctic Oscillation (AO) as found in earlier studies, while trends in ND appear to resemble a trend toward the low-index polarity of the AO. In the Tropics, the Hadley circulation shows significant intensification in both ND and FM, with stronger intensification in FM. Unlike the Hadley cell, the Ferrel cell shows opposite trends between ND and FM, with weakening in ND and strengthening in FM. Comparison of the observational results with general circulation model simulations is also discussed.

1. Introduction

Recent studies showed noticeable trends in Northern Hemisphere (NH) winter and springtime [e.g., January–February–March (JFM)] during the past few decades. Surface air temperatures over the NH high-latitude continents warmed several degrees (Hurrell 1995; Jones et al. 1999; Thompson et al. 2000). The stratospheric Arctic experienced strong cooling in late winter and spring, likely associated with Arctic ozone depletion (Pawson and Naujokat 1999; Randel and Wu 1999; Labitzke and Naujokat 2000). The stratospheric polar night jet strengthened (Waugh et al. 1999), corresponding to decreased wave activity in the extratropics in both the troposphere and the stratosphere (Zhou et al. 2001; Randel et al. 2002; Hu and Tung 2003). It was suggested that these trends from the surface to the stratosphere are dynamically linked through troposphere–stratosphere interaction and that they are closely related to the Arctic Oscillation (AO; Thompson et al. 2000; Hartmann et al. 2000; Wallace and Thompson 2002). These studies, together with others (Baldwin and Dunkerton 2001; Kodera and Kuroda 2000; Hu and Tung 2003; Coughlin and Tung 2005), have emphasized the possible dynamical influence of the stratosphere on the troposphere.

Various general circulation model (GCM) simulation studies have been conducted to address the question of what external forcing mechanisms could be responsible for these observed trends. These studies have mainly focused on testing three possible forcing mechanisms "external" to the atmosphere: increasing greenhouse gases (Shindell et al. 1999; Gillett et al. 2002; Butchart et al. 2000), stratospheric ozone depletion (Graf et al.

Corresponding author address: Dr. Yongyun Hu, Department of Atmospheric Sciences, Peking University, Beijing 100871, China. E-mail: yyhu@pku.edu.cn

1998; Volodin and Galin 1999), and tropical sea surface temperature (SST) warming (Hoerling et al. 2001; Schneider et al. 2003). These simulation studies are primarily interested in the radiative effects from changes in atmospheric trace gases or from changes in tropical sea surface temperatures on atmospheric circulations and regional climate and are concerned with the impact of the Tropics on the extratropics and the influence of the stratosphere on the troposphere.

Decadal trends are also found in early winter months, November–December (ND). Although mainly focusing on the decadal trends in JFM, Zhou et al. (2001), Randel et al. (2002), and Hu and Tung (2003) also commented on the trends in ND. Zhou et al. (2001) showed that wave activity in ND displays trends opposite to that in JFM. Similar results were also reported by Randel et al. (2002). In contrast to intensive studies on the trends in JFM, trends in early winter months have received little attention. Our main goal in this study is to make a closer comparison of decadal trends in various fields and to demonstrate their striking contrast between early winter and late-winter months. It turns out that January is a transition month, from early-winter to late-winter trends. So to contrast the two periods, 2-month averaging without January is used here, that is, ND versus February–March (FM) averages. However it is well known that there is a large intraseasonal vacillation cycle of about 2 months in stratospheric data (Holton and Mass 1976). This cycle was largely eliminated in our earlier studies through 3-month averaging. Here we expect that the statistical significance of any trends in the proposed 2-month-averaged data will be lower. To lend more support to our results, we attempt to obtain a broader and dynamically consistent picture of both the stratospheric and tropospheric trends, and their interrelationships with various dynamical variables.

In section 2, we describe the data and statistical methods used in this study. In section 3, trends in various fields are presented. In addition to studying trends in temperatures, waves, and zonal-mean flows, we also study trends in surface quantities and trends in mean meridional circulations. In the discussion and conclusions section, we compare the observational results with GCM simulations and discuss the possible causes of the opposite trends between early- and late-winter months.

2. Data and method

In this study, data of surface air temperature (SAT) are from the analysis at the NASA Goddard Institute for Space Studies (Hansen et al. 2001). Data of all other fields are the reanalyses from the National Centers for Environmental Prediction–National Center for Atmospheric Research (NCEP–NCAR). Trends in wave activity are calculated using daily data, and trends in other fields are calculated from monthly data. Linear trends of various fields are computed at grid points in the standard way. Student's *t* tests are carried out to examine statistical significance levels of these trends against interannual variability of these fields. In all figures, *t*-test values 1.7, 2, 3, and 4 are plotted using dashed contours, and contours 1.7 and 2.0 approximately correspond to the 90% and 95% confidence level, respectively. In this study, the linear-trend analysis spans over 25 years from the 1978/79 winter to the 2002/03 winter. Thus, trends for ND and FM are calculated over 1978–2002 and 1979–2003, respectively. This period is chosen for several reasons. First, satellite data is included in NCEP–NCAR reanalysis since 1979, and it is commonly thought that the reanalysis data since 1979 are more reliable. Second, our previous time series analyses showed that temperature and wave activity have a clear turning point around the late 1970s and demonstrate systematic tendencies since that time.

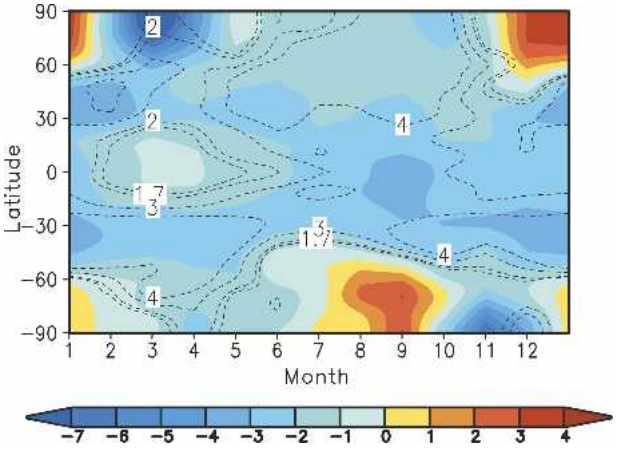

FIG. 1. Twenty-five-year (1978–2002) trends in global zonal-mean temperatures at 50 mb. Color shading interval is 1.0 K per 25 yr. In all figures in this paper, dashed contours indicate Student's *t*-test values for trends.

3. Results

a. Trends in zonal-mean temperature and zonal wind

Figure 1 shows the 25-yr trend in monthly mean zonal-mean temperatures at 50 mb (about 21 km high) as a function of latitudes and months. Overall, Fig. 1 shows that there is general cooling in the stratosphere over the Tropics and extratropics, and these cooling

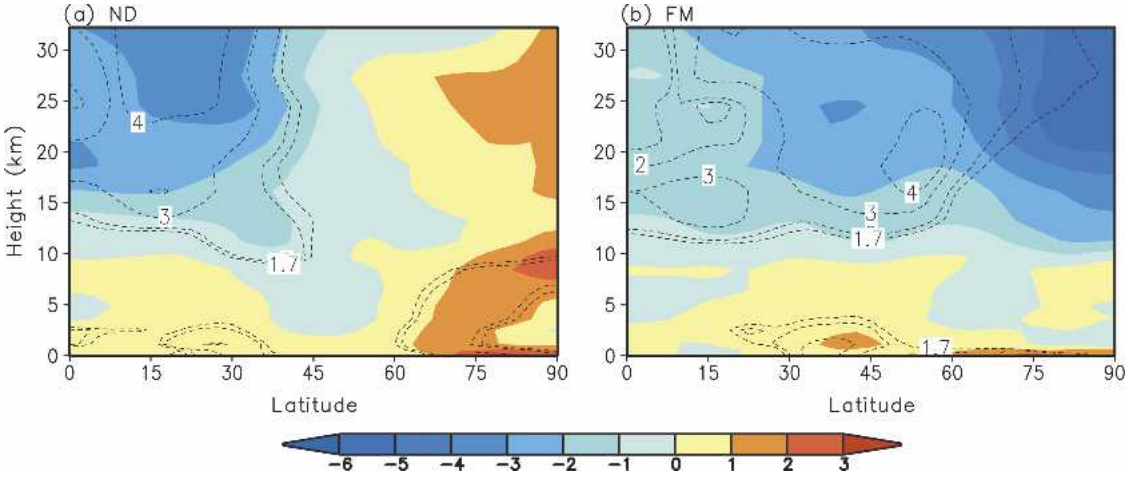

FIG. 2. Trends in zonal-mean temperatures for (a) ND and (b) FM. Color shading interval is 1.0 K per 25 yr.

trends are mostly statistically significant. This is consistent with the radiative effects of greenhouse gas increases and, at midlatitudes during early winter and polar latitudes during late winter, with the radiative cooling due to polar ozone decrease. The exceptional early winter warming of 4 K per 25 yr in the polar regions is however not consistent with the expected effect of radiative changes. They are seen in both the Arctic and the Antarctic in the respective hemisphere's early winter, but the trend is below the 90% confidence level by the Student's *t* test. The cooling trends are particularly strong in late winter and spring (of 5 K per 25 yr) in both polar regions, that is, FM for the Arctic and October–November for the Antarctic.

The timing of the late winter–early spring polar cooling coincides with the period of strong ozone depletion in the polar region when the sun returns. In Hu and Tung (2003) we argued that this cooling is radiatively induced (by the ozone depletion), although there is also the positive feedback of the resultant strong polar vortex inhibiting the propagation of waves into the polar waveguide. The situation in early winter (ND) is different. Since the polar region is in polar night in early winter, most ozone depletion occurs at the edge of the meandering polar vortex, causing smaller but highly statistically significant cooling in the midlatitude stratosphere. The cooling does not extend into the polar region in early winter. The seasonal–spatial pattern in Fig. 1 is close to the results by Ramaswamy et al. (1996) and Randel and Wu (1999) over shorter periods.

Figures 2a and 2b show the meridional–vertical plots of the 25-yr trends in zonal-mean temperatures in ND and FM, respectively. By and large the trends are consistent with the expected effect of increasing greenhouse gases resulting in cooling in the stratosphere and warming in the troposphere with the exception of polar latitudes in early winter, as mentioned previously. In the lower troposphere, especially near the surface, temperatures show significant warming trends in both ND and FM, consistent with the expected warming due to increase in greenhouse gases. In ND, surface significant warming trends in two regions extend to higher levels. One is between about 15° and 40°N, and the other is in the polar troposphere. In FM, the significant warming region is between 20° and 50°N.

Changes in temperatures lead to changes in temperature gradients. Figure 3 shows temperature gradient trends in 25 years. In ND, positive trends, which indicate weakened meridional temperature gradients, are found throughout the lower stratosphere in the extratropics, with high statistical significance over the midlatitudes. The positive trends in temperature gradient are more dynamically relevant than the temperature itself and are known to be conducive to propagation of planetary waves, as we will show later. We therefore suggest that the warming in the polar stratosphere in ND is probably caused by planetary wave dynamical heating. The normally large variability of wave activity is consistent with large variability of the polar warming observed and is consistent with the latter trend not being statistically significant. In late winter, for FM average, there is no significant trend in the temperature gradient over the past 25 years.

Figures 4a and 4b show the 25-yr trends in zonal-mean zonal winds for ND and FM, respectively. These trends are mostly opposite between early and late winter. For ND, negative trends are found throughout the stratosphere jet region and in the subpolar troposphere, with maximum of about -7 m s^{-1} for the 25 years. The statistically significant zonal-wind deceleration is con-

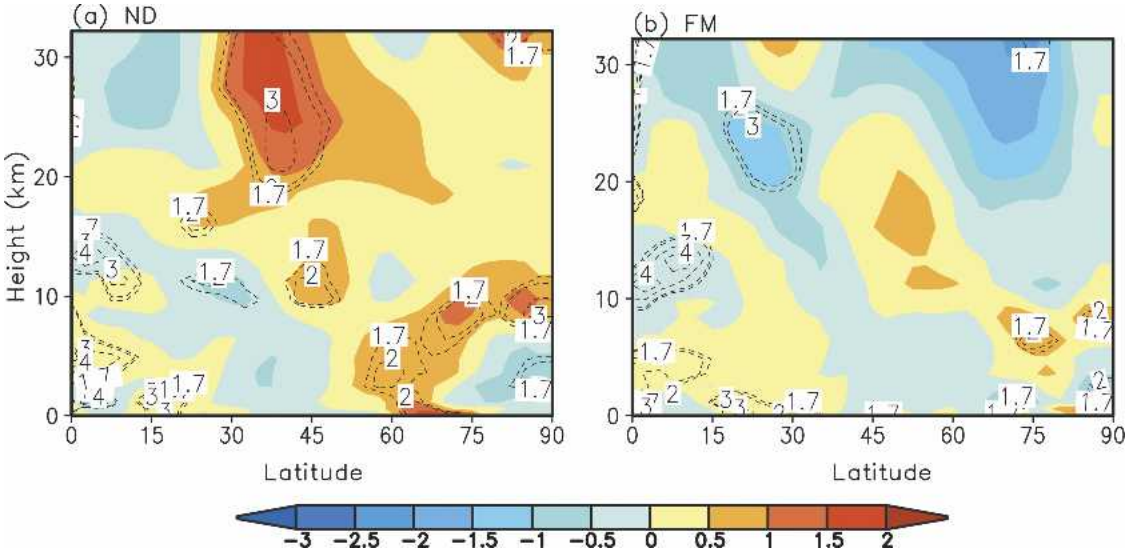

FIG. 3. Trends in zonal-mean temperature gradients for (a) ND and (b) FM. Color shading interval is 1.0×10^{-6} K m^{-1} per 25 yr.

sistent with the weakening of meridional temperature gradients in Fig. 3, according to the thermal wind relation. For FM, a band of mean zonal-wind acceleration extends from the subpolar stratosphere to the midlatitude troposphere. The jet acceleration in the troposphere has significance levels above the 90% confidence level, while the part in the stratosphere, though strong, is not statistically significant for the 2-month average used here.

b. Trends in wave propagation and fluxes

In Hu and Tung (2002, 2003), we focused on time series analyses of wave activity at high latitudes, that is, north of 50°N. Here we show the spatial pattern of EP flux trends in both vertical and meridional directions. We first study the changes in wave propagation. Changes in wave propagation can be anticipated from the trends in the squared indices of refraction (Andrews et al. 1987), although it is difficult to infer which is the cause and which is the effect. Regions with positive trends in the indices of refraction tend to be more favorable for wave propagation, while the regions with negative trends tend to refract waves away. Figure 5a shows the trends in wavenumber-1 refractive indices for ND. Positive trends are in the subpolar troposphere and most parts of the stratosphere, with a maximum near the subpolar tropopause. Such a spatial distribution of the refractive index trends suggests that the

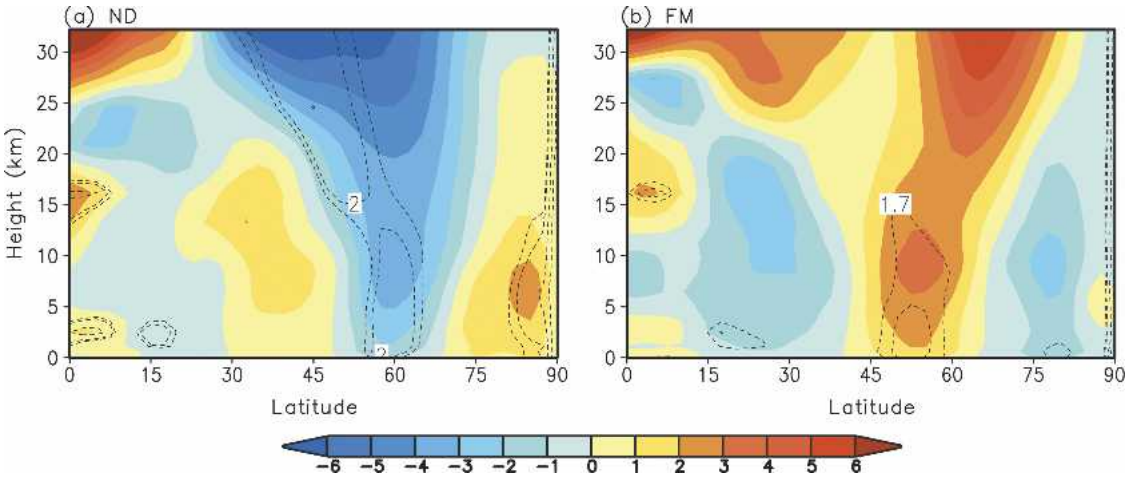

FIG. 4. Trends in zonal-mean zonal winds for (a) ND and (b) FM. Color shading interval is 1.0 m s^{-1} per 25 yr.

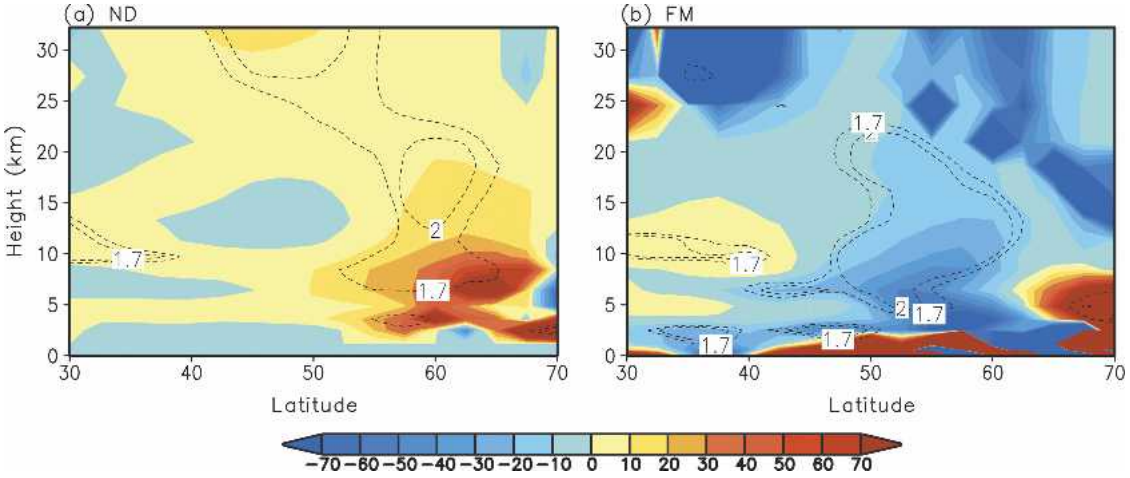

FIG. 5. Trends in squared refractive indices for wavenumber 1 for (a) ND and (b) FM. The index square is multiplied by the square of the earth's radius, a^2. Color interval is 10 m^2 per 25 yr. To avoid extremely large values of the refractive indices in the subtropics and near the pole where the linear wave theory is no longer valid, the plot is limited between 30° and 70°N.

high-latitude extratropics have become more favorable for wave propagation. Thus, planetary waves tend to propagate upward along the subpolar waveguide in ND.

Figure 5b shows the trends in refractive indices for FM. The stratosphere is dominated by negative trends, indicating that in FM the stratosphere has become less favorable for planetary wave propagation in the 25 years. A band of negative trends between 45° and 65°N, with high statistical significance, extends from the stratosphere into the troposphere. Since this region is the primary channel for upward planetary wave propagation, the negative trends suggest suppressed wave propagation from the troposphere into the stratosphere. While the refractive indices exhibit negative trends in high latitudes, they show significant weak positive trends in the upper troposphere at lower latitudes (between 30° and 45°N). Such a spatial pattern, opposite to that in ND, indicates that in FM waves tend to propagate more equatorward than upward and poleward. This late-winter part of the result has previously been demonstrated in Hu and Tung (2003).

The opposite tendencies in wave propagation can be more explicitly demonstrated with trends in Eliassen–Palm (EP) flux vectors, since EP flux vectors approximately point toward the local directions of wave propagation (Andrews et al. 1987). The white arrows in Figs. 6a and 6b denote changes in EP flux vectors over the 25 years. Since the climatological direction of wave propagation in the extratropical troposphere is upward and equatorward, in Fig. 6a the poleward arrows in the middle and upper extratropical troposphere indicate reduced equatorward wave propagation in ND. The upward arrows in the mid- and high-latitude stratosphere represent enhanced upward wave propagation from the troposphere to the stratosphere. In Fig. 6b, the downward arrows in the polar region indicate suppressed upward wave propagation at high latitudes, and the equatorward and upward arrows in the midlatitude upper troposphere indicate enhanced wave propagation toward the subtropical upper troposphere. Indeed, the trends in EP flux vectors are consistent with the trends in the refractive indices. Such opposing tendencies in wave propagation between early and late-winter months were also reported by Zhou et al. (2001).

As wave propagation is altered, EP flux divergence, which characterizes the interaction between waves and the zonal-mean flow, may also be changed. The trends in EP flux divergence in ND and FM are shown in Figs. 6a and 6b (background color shading), respectively. In ND, the stratosphere between 45° and 90°N is dominated by the negative trends, indicating increased EP flux convergence in the mid- and high-latitude stratosphere consistent with wave heating of the polar region shown in Fig. 2a. Positive trends are located in the lower-latitude stratosphere. In the troposphere, the situation is complicated. Nevertheless, one can find negative trends in the upper troposphere between 50° and 70°N and positive trends in the middle troposphere between 30° and 50°N. These roughly correspond to the zonal-wind changes in the troposphere shown in Fig. 4a.

For FM, positive trends in EP flux divergence (less convergence), with high significance, are in the high-latitude stratosphere. Negative trends (more convergence) are in lower latitudes (between about 30° and 55°N). This is opposite to that in ND. In the tropo-

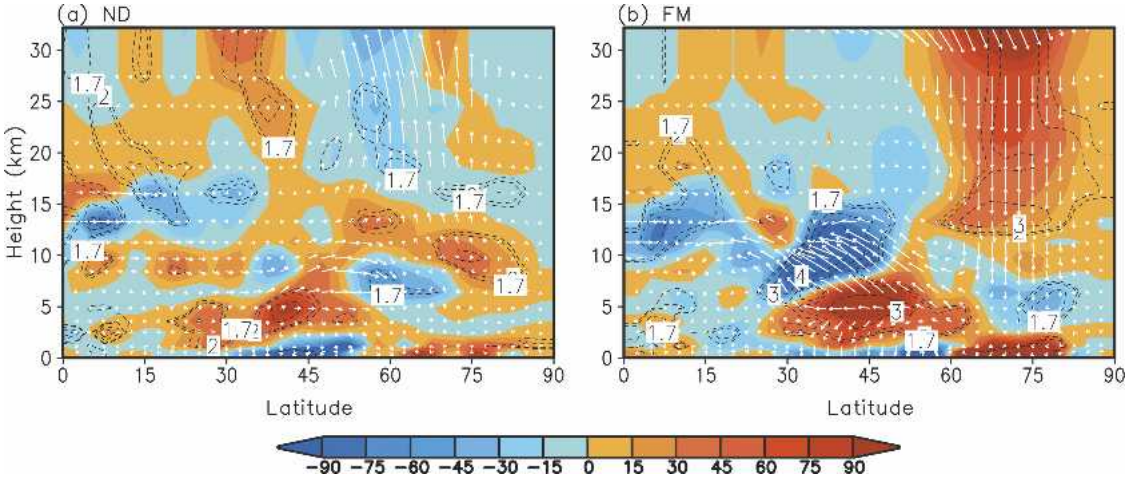

FIG. 6. Trends in EP fluxes for (a) ND and (b) FM. The white arrows denote trends in EP flux vectors, and the color shading indicates trends in EP flux divergence. Both EP flux vectors and EP divergence are divided by the background air density to make them visible at high levels. The scaling length of the arrows, 2.54 cm or 1 in., represents 1.0×10^8 $m^3 s^{-2}$ per 25 yr. To illustrate the changes in EP fluxes in the vertical direction, the vertical component of EP fluxes is multiplied by 100. Color interval of the trends in EP flux divergence is 15 $m^2 s^{-2}$ per 25 yr. Dashed contours indicate Student's *t*-test values for the trends in EP flux divergence.

sphere, positive trends are located in the middle troposphere between 25° and 60°N. Large negative trends are in the upper troposphere between 25° and 45°N, indicating largely enhanced EP flux convergence. These positive and negative trends correspond to the zonal-wind acceleration at subpolar latitudes and deceleration in the subtropics, respectively, as shown in Fig. 4b.

Thus, it is seen that there is a general consistency between stratospheric polar warming, zonal jet deceleration, and enhanced wave drag in the stratosphere in ND, with the reversed situation in FM: There is again a general consistency between polar cooling, zonal jet acceleration, and reduced wave drag in FM. In Hu and Tung (2003), we argued that for late winter, defined then as JFM average, it is possibly the polar ozone depletion that is the cause of the cooling trend since 1979 in the polar stratosphere and that the reduced wave drag is the result of altered index of refraction due to the polar cooling. We stand by that interpretation for the late-winter result reported here for FM.

c. *Trends in mean meridional circulations*

Most earlier studies on wintertime climate trends in the Northern Hemisphere focused on circulation changes in the zonal direction and their interaction with waves. Here, we show that significant trends are also found for zonal-mean meridional circulations. First, let us look at the trends in zonal-mean meridional winds (Fig. 7). In the Tropics in ND, significant positive trends are found around the tropical tropopause, and negative trends are located in the middle and lower tropical troposphere, with statistical significance above 95%. In the extratropics, trends are generally positive, except for negative trends near the extratropical surface between 45° and 65°N. For FM, a band of strong and significant positive trends is around the tropical tropopause and lower stratosphere with negative trends in the middle and lower tropical troposphere. Statistical significance levels of these trends are above the 95% confidence level. In the extratropics, negative trends are in the middle and upper troposphere, and the positive trends are near the surface between 40° and 65°N, opposite to that in ND.

Figures 8a and 8b show trends in zonal (Eulerian) mean mass streamfunction for ND and FM, respectively. To show the changes in the Hadley circulation across the equator, the plots are extended to 45°S. In calculating the mass streamfunction, a negative sign is defined for clockwise circulation in the meridional–vertical plane. Therefore, in Figs. 8a and 8b the negative trends over the equator and the northern Tropics indicate intensification of the northern branch of the Hadley circulation, and the positive trends over the southern Tropics indicate intensification of the southern branch. In ND, the intensification of the Hadley cell occurs mainly in the middle and upper tropical troposphere, while the lower part of the Hardley cell shows some weakening. In FM, the overall Hadley cell is intensified, and the intensification is much stronger than in ND. The maximum increase of the mass streamfunc-

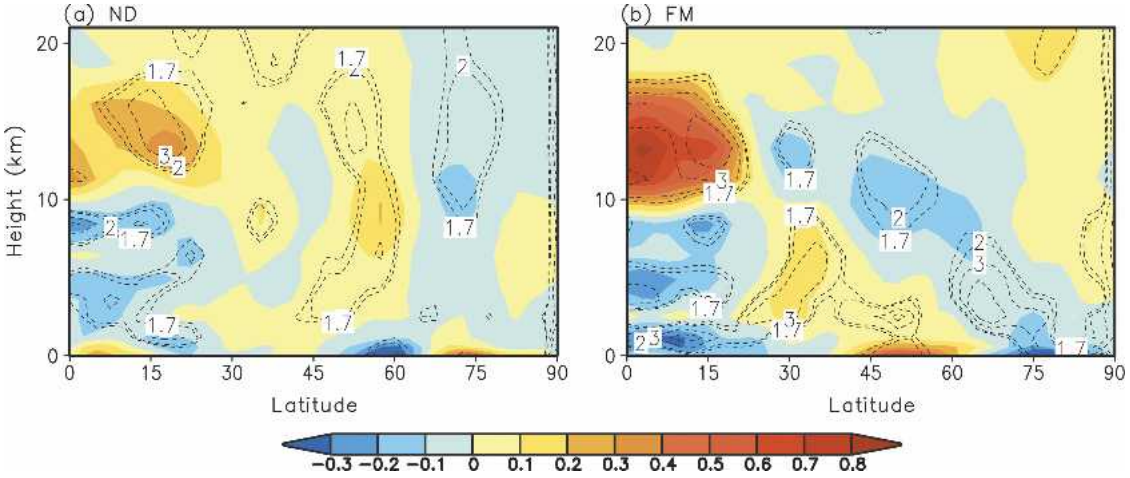

FIG. 7. Trends in zonal-mean meridional winds for (a) ND and (b) FM. Color shading interval is 0.1 m s^{-1} per 25 yr.

tion in FM is greater than 40×10^9 kg s^{-1} for the 25 years, which is about 29% of the climatological maximum streamfunction in FM (about 140×10^9 kg s^{-1}). It is likely that the intensification of the Hadley cell in both ND and FM is related to the observed tropical SST warming. Using independent datasets, Kumar et al. (2004) showed positive trends in tropical precipitation and surface temperatures since the late 1970s. In the extratropics, trends in mass streamfunction are negative in ND and positive in FM. Since the climatological Ferrel cell corresponds to positive streamfuctions, these extratropical trends indicate that the Ferrel cell is weakened in ND but strengthened in FM. Since it is known that the Ferrel cell is a wave-driven, thermally indirect, meridional circulation (Holton 1992), the opposite trends in the Ferrel cell between ND and FM are presumably due to the opposite tendencies in tropospheric midlatitude wave fluxes in Fig. 6.

d. Trends near the surface

Opposite trends between ND and FM are also found near the surface. Figures 9a and 9b show the 25-yr SAT trends for ND and FM derived from the SAT analysis at the NASA/Goddard Institute for Space Studies (Hansen et al. 2001). In ND, the SAT trends exhibit cooling over the high-latitude Europe–Asia continent. Maximum cooling of about −4°C for the 25 years is over Siberia, with significance above the 90% confidence level. Significant warming trends in ND are over the Arctic polar region, particularly over Greenland and northern Canada. In contrast, as shown in many earlier studies (Hurrell 1995; Jones et al. 1999; Thomp-

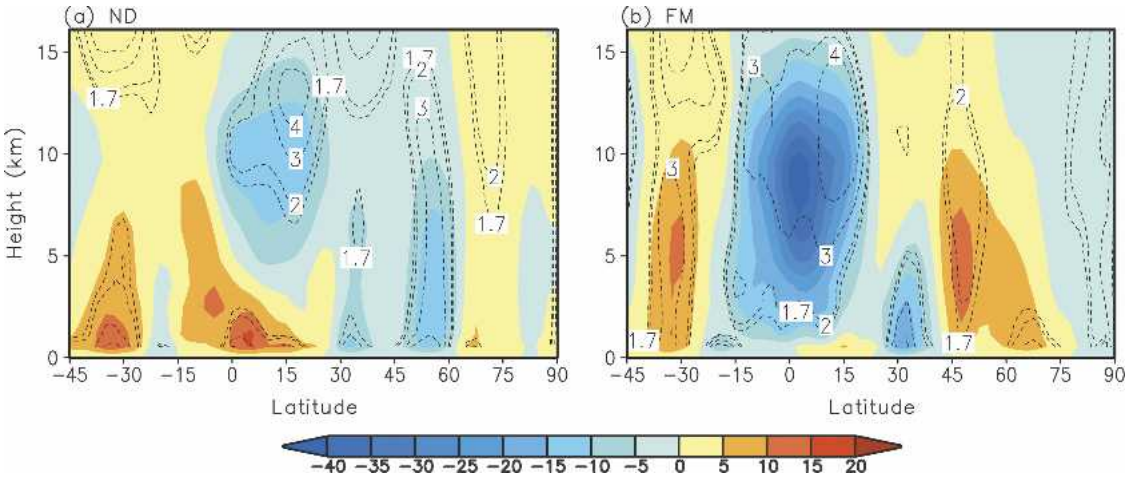

FIG. 8. Trends in mean meridional mass streamfunction for (a) ND and (b) FM. Color shading interval is 5×1.0^9 kg s^{-1} per 25 yr.

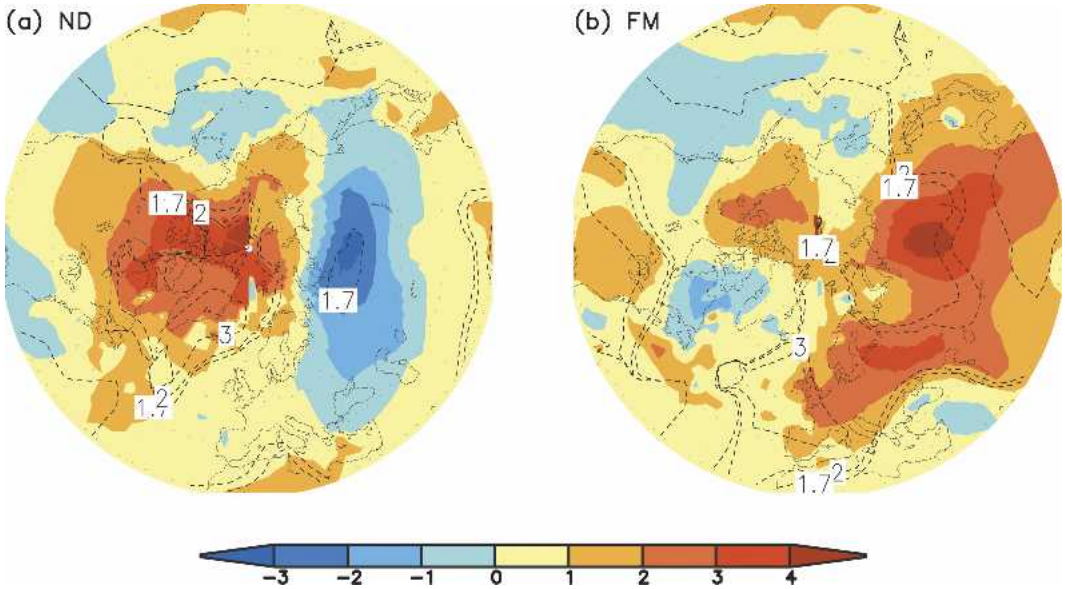

FIG. 9. Trends in SATs for (a) ND and (b) FM. Color interval is 1.0 K per 25 yr.

son et al. 2000), in FM SATs display warming trends over the high-latitude Europe–Asia continent and cooling trends over northeastern Canada. The spatial pattern of SAT trends over high latitudes shows striking contrast between ND and FM. The early winter cooling trends have magnitudes comparable to that of the warming trends in FM. Linear trends from NCEP–NCAR analysis show similar results (figure not shown).

Figures 10a and 10b show the 25-yr trends in sea level pressure (SLP) for ND and FM. For ND, positive trends are mainly over the high-latitude Europe–Asia continent and part of the Arctic Ocean, with maxima over northern Europe and Russia. Negative trends are over the extratropical Atlantic, North America, and the Pacific. There are two negative maxima, one over the North Atlantic and the other one over the North Pacific. For FM, negative trends are over the high-latitude Europe–Asia continent with a maximum over northern Europe and Russia, and positive trends are mainly over the extratropical oceans. The SLP trends clearly show opposite spatial patterns between ND and FM. It was shown in earlier studies (e.g., Thompson et al. 2000)

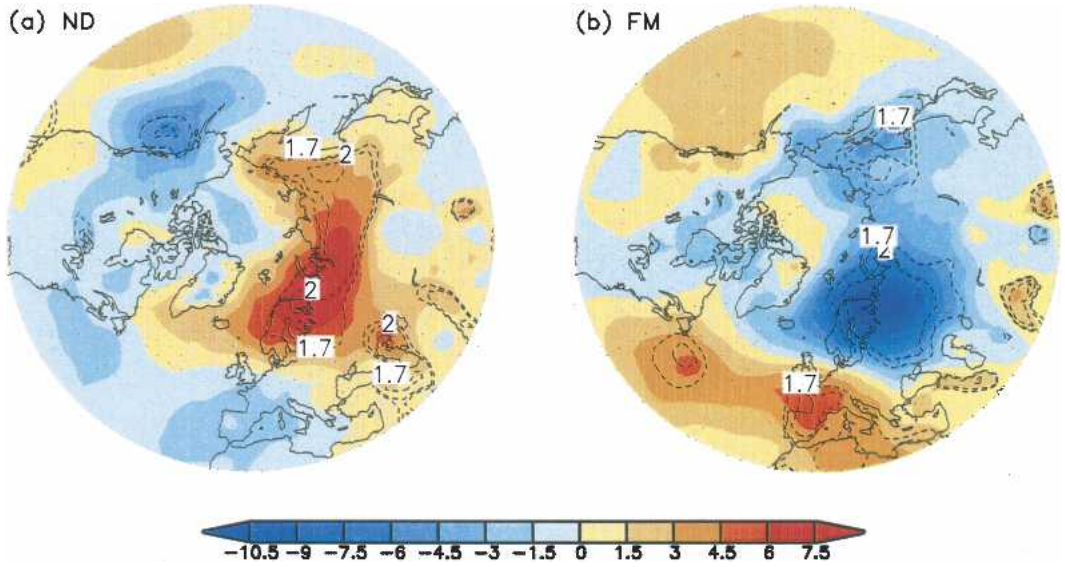

FIG. 10. Trends in SLP for (a) ND and (b) FM. Color shading interval is 1.5 mb per 25 yr.

that the SLP trends in FM are associated with a positive AO trend. This implies that the SLP trends in ND are related to a negative AO trend (the AO index in ND in fact exhibits a weak negative trend over 1978–2002). Moreover, the spatial pattern of the SLP trends in ND suggests a tendency toward the Eurasian blocking. Thompson and Wallace (2001) pointed out that, when the AO is in the low-index phase, it is more likely to form blocking systems and that blocking systems slow down the usual eastward propagation of weather systems, lead to intrusion of cold polar air over high-latitude continents, and cause cooling. They showed that during 1958–97 blocking days in the low-index AO phases over Russia are about three times of that in the high-index AO phases (82 days versus 29 days). This suggests that the continental cooling in ND is related to the increase of Eurasian blocking days (events) upstream. The tendency toward blocking in ND leads to a local enhancement of southward motion over the Europe–Asia continent.

The trends near the surface may be dynamically linked to the trends aloft. Wallace and Thompson (2002) have commented that the continental warming in late winter and springtime is related to the acceleration of extratropical zonal winds. From Fig. 4b, one can find that the zonal-wind acceleration extends from the stratosphere to the surface. Wallace and Thompson (2002) also pointed out that when the AO is in the low-index phase, mean zonal winds are weaker or zonal flows are meandering and that broader meanders aloft are likely to form blocking systems. From Fig. 4a, we have seen that the zonal-wind deceleration extends from the stratosphere to the troposphere. It is expected that the SLP tendency toward blocking in ND has a close relation to the zonal-wind deceleration aloft.

The blocking signature is usually characterized using 500-mb geopotential heights (D'Andrea et al. 1998). To further demonstrate the tendency toward blocking in ND, and to compare the trends in geopotential heights between ND and FM, we plot the trends in geopotential heights at three levels: 500, 100, and 50 mb. Figure 11a shows the 25-yr trends in geopotential heights at 500 mb in ND. In general, the polar region shows positive trends, while the extratropics is dominated by negative trends. The maximum positive trends are over northern Europe, with statistical significance above the 90% or 95% confidence level. The maximum positive trends are indicative of the tendency toward blocking. Comparison of Fig. 11a with Fig. 10a shows westward and poleward tilting with height of the positive trends. At 100 and 50 mb, positive trends are also in the polar region with maximum trends shifting over the opposite side of the Arctic. However, the positive trends at these levels are less significant. For FM, at 500 mb the maxima of significant negative trends are over northern Europe with significant positive maxima over North Atlantic and western Europe. This is opposite to that in ND. With increasing height, the negative maxima shift eastward from northern Europe to northeastern Russia. In addition, the trends at 100 and 50 mb show a dipole structure. The results here suggest a strong vertical coherence of trends.

4. Discussion and conclusions

We have compared the recent decadal trends in various fields between ND and FM. In the Tropics, the Hadley circulation exhibits significant intensification in both ND and FM, with much stronger intensification occurring in FM. In the extratropics and polar region, trends and their spatial structures are nearly opposite between the early and late winter months. In ND, the trends are characterized by decelerated mean zonal winds, weakened Ferrel cell, enhanced upward wave fluxes associated with reduced equatorward wave fluxes, warming in the stratosphere polar region, and SAT cooling over the high-latitude Europe–Asia continent related to the tendency toward Eurasia blocking. In FM, the trends show accelerated zonal winds, strengthened Ferrel cell, reduced upward wave fluxes in both the high-latitude stratosphere and troposphere accompanied by enhanced equatorward wave fluxes in the extratropical troposphere, cooling in the polar troposphere and stratosphere, and SAT warming over the high-latitude Europe–Asia continent. The trends in FM are associated with an AO trend toward the high-index polarity, as suggested by earlier studies. While the trends in ND appear to resemble a tendency toward the low-index AO polarity, the magnitudes of trends in ND are slightly weaker than that in FM.

It should be pointed out that Kinter et al. (2004) found that the NCEP–NCAR reanalysis has an apparent interdecadal shift in the tropical divergent circulation around the middle 1970s and suggested that the shift may be an artifact of changes in data assimilation procedures. Kanamitsu et al. (2002) reported some human processing errors in the NCEP–NCAR reanalysis. Whether and how these errors impact the above trends needs further studies. Our preliminary results of trends from the reanalysis of the European Centre for Medium-Range Weather Forecasts show similar magnitudes and spatial patterns (results not shown here).

What causes the opposite trends between early and late winter months? Comparison of the observed trends with existing GCM simulation results may be helpful for understanding this question. Hou (1998) demon-

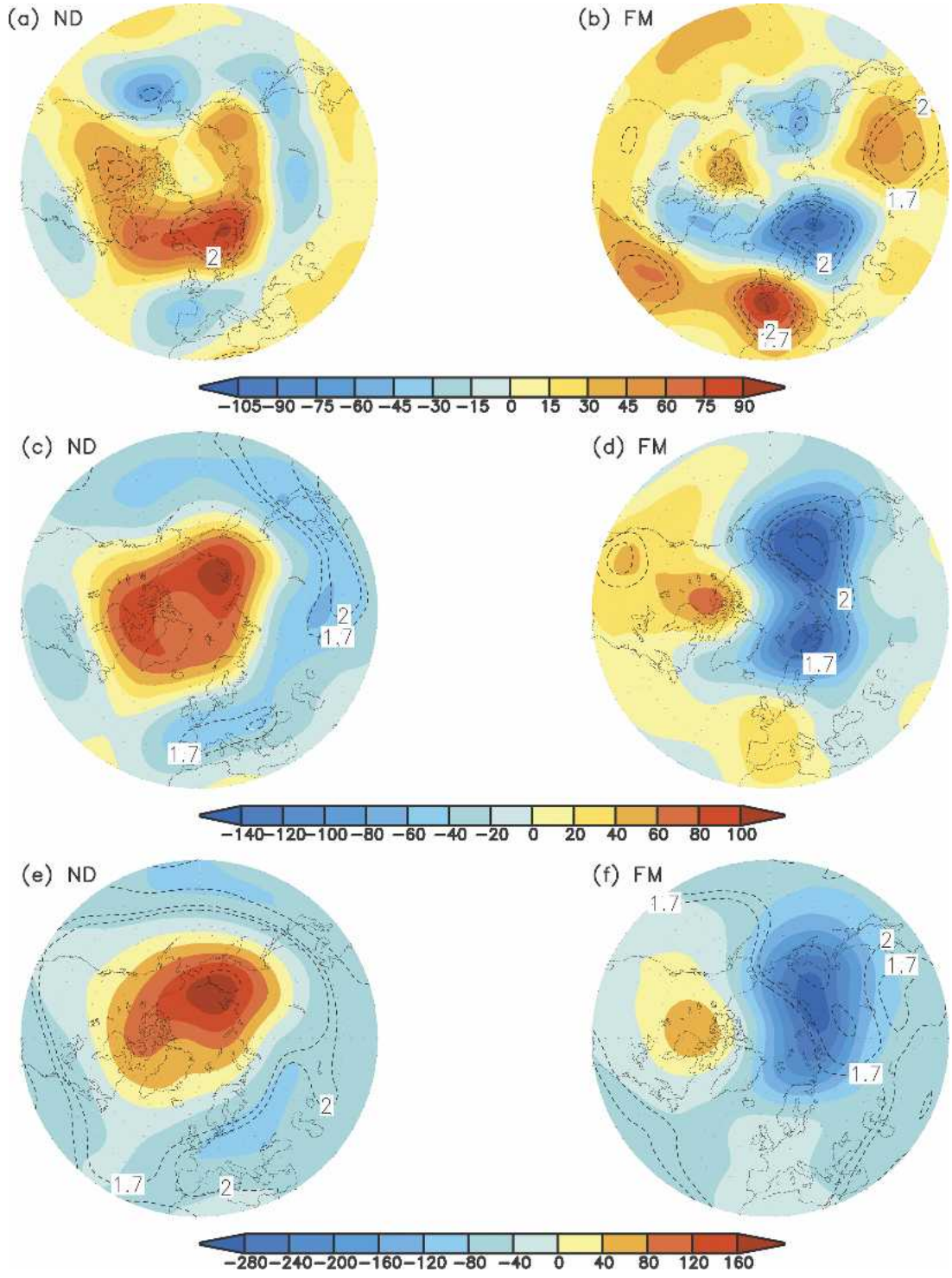

FIG. 11. Trends in geopotential heights for (left) ND and (right) FM. The plots show trends in geopotential heights at (a), (b) 500, (c), (d) 100, and (e), (f) 50 mb. Units for the color shading intervals are meters per 25 yr.

strated that, as the Tropics is warmed, the Hadley cell is intensified. The stronger Hadley cell transports more angular momentum to the subtropics, thus accelerating the subtropical jet. The stronger jet then leads to increased wave activity and EP flux convergence in the extratropical troposphere, which decelerates zonal winds there. Meanwhile, the increase of wave activity enhances eddy heat transport from midlatitudes to the

polar region and causes midlatitude tropospheric cooling and polar warming. The similarity between the observations and simulations suggests a possible impact of the Tropics on the extratropics due to the intensification of the Hadley circulation. The observed early-winter trends are also partly similar to the GCM simulation results by Butchart et al. (2000) and Robinson et al. (2002). Butchart et al. (2000) showed that increasing greenhouse gases lead to increased wave activity at mid- and high latitudes and warming in the polar region in both the troposphere and stratosphere during winter months. Robinson et al. (2002) showed that, as an observed time-varying SST anomaly is forced in a GCM, the tropical troposphere shows warming and the extratropical upper troposphere responds with cooling and enhanced planetary wave activity in wintertime. The consistency between the above observations in ND and simulations suggests that the early winter tropospheric trends in the extratropics and high latitudes might be responses to tropical SST warming.

However, the above consistency fails for FM when the even stronger intensification of the Hadley circulation is accompanied by a decelerated subtropical tropospheric jet and reduced wave activity in the mid- and high latitudes in late winter. There have been GCM simulation studies to test whether the late-winter trends are caused by increasing greenhouse gases, tropical SST warming, or stratospheric Arctic ozone depletion. For ozone depletion, while Volodin and Galin (1999) showed that the anomalous continental warming in the early 1990s could be reproduced by imposing observed ozone trend in their GCM, Graf et al. (1998) showed that over a longer time period (1979–97) surface responses to imposed Arctic ozone depletion are weaker than the observed trends and that the surface responses occur in April and May, about 2 months later than observed surface trends. The delay of Arctic cooling was also found by Ramaswamy et al. (1996) and Langematz et al. (2003). In these simulations, the Arctic cooling rate in the lower stratosphere, about -2 K per 20 yr, is also much weaker than the observed cooling rate of about -5 K or -6 K per 25 yr. Therefore, it remains unclear whether the radiative effect of stratospheric ozone depletion alone is sufficient in generating the observed trends in late winter and spring.

Shindell et al. (1999) showed that increasing greenhouse gases is able to generate a positive AO trend comparable to the observed AO trend. They proposed that the increase in greenhouse gases causes warming in the tropical and midlatitude troposphere and cooling in the stratosphere, which enhances the meridional temperature gradient near the midlatitude tropopause. The enhancement of temperature gradients leads to accelerated zonal winds in the extratropics, which tend to refract planetary waves equatorward, and cause a positive AO trend and continental warming. Gillett et al. (2002) compared simulation results from different GCMs (see their Table 1). They found that in most of these GCMs increasing greenhouse gases lead to an AO trend weaker than observations. They also found that some GCMs either could not produce an AO trend or produced a negative AO trend. Butchart et al. (2000) showed that increasing greenhouse gases lead to increased wave activity at mid- and high latitudes and warming in the polar troposphere and stratosphere, which implies a negative AO trend. As mentioned earlier, this appears to be similar to the observed patterns in early winter.

Model simulations with tropical SST forcing also yielded conflicting results. While Hoerling et al. (2001) showed that tropical SST warming leads to a positive trend in the North Atlantic Oscillation (NAO) with negative geopotential height trends in the polar region and positive geopotential height trends in the extratropics, Schneider et al. (2003) found no significant AO or NAO trends in geopotential heights from tropical SST forcing. Moreover, Robinson et al. (2002) showed that tropical SST forcing generates a Pacific–North American pattern in the winter season with positive trends in geopotential heights in the polar region and negative trends in the extratropics, which is nearly opposite to the results by Hoerling et al. (2001). Butchart et al. (2000) and Schneider et al. (2003) speculated that these divergent results on the effects of increasing greenhouse gases and tropical SST forcing might be model dependent. In the simulation results discussed above, the forcing effects were tested separately. In the real climate system, tropical SST warming is very likely related to increasing greenhouse gases, rather than an independent forcing. Using a coupled atmosphere–ocean GCM, Fyfe et al. (1999) have tested how increasing greenhouse gases influence the AO trends and found no significant AO trend until after year 2020, when the forced CO_2 concentration is much higher than present (some of the simulation results in Gillett et al. (2002) are also from coupled ocean–atmosphere GCMs.)

The meridional structure of the observed temperature trends in Fig. 2b seems not to be consistent with the proposed mechanism that the extratropical and high-latitude trends in FM are related to tropical warming due to either increasing greenhouse gases or tropical SST warming. First, Fig. 2b shows weak cooling trends in the middle and upper tropical troposphere, rather than warming. Second, the midlatitude warming in the upper troposphere, in contrast to the cooling in

nearly the same region in ND, is related to enhanced eddy heat fluxes from the subtropics to midlatitudes and is not necessarily a result of greenhouse warming. The disagreements or nearly opposite results of these GCM simulations and the inconsistency between the simulations and observations leave unanswered the question of how increasing greenhouse gases and tropical SST warming can lead to climate changes in the extratropics and high latitudes in FM.

We are not aware of simulations reporting a contrast of trends between ND and FM as we have found. One reason is probably because most of these studies used the conventional seasonal average, that is, averaging over December–February. Such a seasonal averaging would obviously obscure the contrast of trends between early winter and late-winter months. Therefore, it is important for future simulations to separately test the possible forcing for trends in early winter and late-winter months. Considering that the effects of increasing greenhouse gases or tropical SST warming persist all winter, it is even more important to identify whether and how these forcing mechanisms can possibly lead to different trends between early winter and late-winter months and to understand how late-winter trends are dynamically linked to trends in early winter months.

Acknowledgments. Hu is supported by the NASA Goddard Institute for Space Studies. K. K. Tung's research is supported by the NSF under Grants ATM01-32737 and ATM98-13770. NCEP–NCAR reanalysis data are provided by the NOAA–CIRES Climate Diagnostics Center, Boulder, Colorado, from their Web site (http://www.cdc.noaa.gov/).

REFERENCES

Andrews, D. G., J. R. Holton, and C. B. Leovy, 1987: *Middle Atmosphere Dynamics.* Academic Press, 489 pp.

Baldwin, M. P., and T. J. Dunkerton, 2001: Stratospheric harbingers of anomalous weather regimes. *Science,* **294,** 581–584.

Butchart, N., J. Austin, K. R. Knight, A. A. Scaife, and K. L. Gallani, 2000: The response of the stratospheric climate to projected changes in the concentrations of well-mixed greenhouse gases from 1992 to 2051. *J. Climate,* **13,** 2142–2159.

Coughlin, K., and K. Tung, 2005: Tropospheric wave response to descending decelerations in the stratosphere. *J. Geophys. Res.,* **110,** D01103, doi:10.1029/2004JD004661.

D'Andrea, F., and Coauthors, 1998: Northern Hemisphere atmospheric blocking as simulated by 15 atmospheric general circulation models in the period 1979–1988. *Climate Dyn.,* **14,** 385–407.

Fyfe, J. C., G. J. Boer, and G. M. Flato, 1999: The Arctic and Antarctic oscillations and their projected changes under global warming. *Geophys. Res. Lett.,* **26,** 1601–1604.

Gillett, N. P., and Coauthors, 2002: How linear is the Arctic Oscillation response to greenhouse gases? *J. Geophys. Res.,* **107,** 4022, doi:10.1029/2001JD000589.

Graf, H.-K., I. Kirchner, and J. Perlwitz, 1998: Changing lower stratospheric circulation: The role of ozone and greenhouse gases. *J. Geophys. Res.,* **103,** 11 251–11 261.

Hansen, J. E., and Coauthors, 2001: A closer look at United States and global surface temperature change. *J. Geophys. Res.,* **106,** 23 947–23 963.

Hartmann, D. L., J. M. Wallace, V. Limpasuvan, D. J. W. Thompson, and J. R. Holton, 2000: Can ozone depletion and greenhouse warming interact to produce rapid climate change? *Proc. Natl. Acad. Sci. USA,* **97,** 1412–1417.

Hoerling, M. P., W. Hurrell, and T. Xu, 2001: Tropical origins for recent North Atlantic climate change. *Science,* **292,** 90–92.

Holton, J., 1992: *An Introduction to Dynamic Meteorology.* 3d ed. Academic Press, 511 pp.

——, and C. Mass, 1976: Stratospheric vacillation cycles. *J. Atmos. Sci.,* **33,** 2218–2225.

Hou, A., 1998: Hadley Circulation as a modulator of the extratropical climate. *J. Atmos. Sci.,* **55,** 2437–2457.

Hu, Y., and K. Tung, 2002: Interannual and decadal variations of planetary wave activity, stratospheric cooling, and Northern Hemisphere annular mode. *J. Climate,* **15,** 1659–1673.

——, and ——, 2003: Possible ozone-induced long-term changes in planetary wave activity in late winter. *J. Climate,* **16,** 3027–3038.

Hurrell, M., 1995: Decadal trends in the North Atlantic Oscillation region temperatures and precipitation. *Science,* **269,** 676–679.

Kanamitsu, M., W. Ebisuzaki, J. Woollen, S. Yang, J. J. Hnilo, M. Fiorino, and G. L. Potter, 2002: NCEPDOE AMIP-II Reanalysis (R-2). *Bull. Amer. Meteor. Soc.,* **83,** 1631–1643.

Kinter, J. L., M. J. Fennessy, V. Krishnamurthy, and L. Marx, 2004: An evaluation of the apparent interdecadal shift in the tropical divergent circulation in the NCEP–NCAR reanalysis. *J. Climate,* **17,** 349–361.

Kodera, K., and H. Kuroda, 2000: Tropospheric and stratospheric aspects of the Arctic Oscillation. *Geophys. Res. Lett.,* **27,** 3349–3352.

Kumar, A., F. Yang, L. Goddard, and S. Schubert, 2004: Differing trends in the tropical surface temperatures and precipitation over land and oceans. *J. Climate,* **17,** 653–664.

Jones, P. D., M. New, D. E. Parker, S. Martin, and I. G. Rigor, 1999: Surface air temperature and its changes over the past 150 years. *Rev. Geophys.,* **37,** 173–199.

Labitzke, K., and B. Naujokat, 2000: The lower Arctic stratosphere in winter since 1952. *SPARC Newsletter,* No. 15, SPARC Office, Toronto, ON, Canada, 11–14.

Langematz, U., and Coauthors, 2003: Thermal and dynamical changes of the stratosphere since 1979 and their link to ozone and CO_2 changes. *J. Geophys. Res.,* **108,** 4027, doi:10.1029/2002JD0002069.

Pawson, S., and B. Naujokat, 1999: The cold winter of the middle 1990s in the northern lower stratosphere. *J. Geophys. Res.,* **104,** 14 209–14 222.

Ramaswamy, V., M. D. Schwarzkopf, and W. J. Randel, 1996: Fingerprint of ozone depletion in the spatial and temporal pattern of recent lower-stratospheric cooling. *Nature,* **382,** 616–618.

Randel, W. J., and F. Wu, 1999: Cooling of the Arctic and Antarctic polar stratospheres due to ozone depletion. *J. Climate,* **12,** 1467–1479.

——, ——, and R. Stolarski, 2002: Changes in column ozone correlated with the stratospheric EP flux. *J. Meteor. Soc. Japan,* **80,** 849–862.

Robinson, W. A., R. Reudy, and J. E. Hansen, 2002: General circulation model simulations of recent cooling in the east-central United States. *J. Geophys. Res.,* **107,** 4748, doi:10.1029/200IJD001577.

Schneider, E. K., L. Bengtsson, and Z. Hu, 2003: Forcing of Northern Hemisphere climate trends. *J. Atmos. Sci.,* **60,** 1504–1521.

Shindell, D. T., R. L. Miller, G. A. Schmidt, and L. Pandolfo, 1999: Simulation of recent northern winter climate trends by greenhouse-gas forcing. *Nature,* **399,** 452–454.

Thompson, D. W. J., and J. M. Wallace, 2001: Regional climate impacts of the Northern Hemisphere annular mode. *Science,* **293,** 85–89.

——, ——, and G. C. Hegerl, 2000: Annular modes in the extratropical circulation. Part II: Trends. *J. Climate,* **13,** 1018–1036.

Volodin, E. M., and V. Ya. Galin, 1999: Interpretation of winter warming on Northern Hemisphere continents in 1977–94. *J. Climate,* **12,** 2947–2955.

Wallace, J. M., and D. W. J. Thompson, 2002: Annular modes and climate prediction. *Phys. Today,* **55,** 29–33.

Waugh, D. W., W. J. Randel, S. Pawson, P. A. Newman, and E. R. Nash, 1999: Persistence of the lower stratospheric polar vortices. *J. Geophys. Res.,* **104,** 27 191–27 202.

Zhou, S., A. Miller, J. Wang, and J. K. Angell, 2001: Trends of NAO and AO and their associations with stratospheric processes. *Geophys. Res. Lett.,* **28,** 4107–4110.